

## Polyoxometalate Intercalated Layered Double Hydroxide for Degradation of Procion Red

Yulizah Hanifah<sup>1</sup>, Risfidian Mohadi<sup>1,2</sup>, Mardiyanto<sup>3</sup>, Aldes Lesbani<sup>1,2\*</sup>

<sup>1</sup> Graduate School of Mathematics and Natural Sciences, Faculty of Mathematics and Natural Sciences, Universitas Sriwijaya, Jl. Palembang Prabumulih Km.32 Oganllir 30662, Indonesia

<sup>2</sup> Research Center of Inorganic Materials and Coordination Complexes, Faculty of Mathematics and Natural Sciences, Universitas Sriwijaya, Jl. Palembang Prabumulih Km.32 Oganllir 30662, Indonesia

<sup>3</sup> Department of Pharmacy, Faculty of Mathematics and Natural Sciences, Universitas Sriwijaya, Jl. Palembang Prabumulih Km.32 Oganllir 30662, Indonesia

\* Corresponding author's e-mail: [aldeslesbani@pps.unsri.ac.id](mailto:aldeslesbani@pps.unsri.ac.id)

### ABSTRACT

The synthesis and characterization of layered double hydroxide (LDH) and intercalated polyoxometalate were presented. The growth of polyoxometalate on Ni/Mg layered double hydroxide for degradation procion red (PR) was reported. The degradation parameters and organic dye removal efficiency of Zn/Mg-LDH and both composite LDH-polyoxometalate were determined by considering factors such as pH of dye solution, catalyst dosage, and time as variables of degradation. X-Ray, FTIR, and SEM spectroscopy confirmed the layered double hydroxide structure. XRD and FTIR analysis confirmed the single-phase of the as-made and polyoxometalate intercalated LDH. SEM images show the formation of aggregates of small various sizes. The catalytic activity of the material was evaluated in the degradation of PR as a model pollutant. The result showed that MgAl-SiW<sub>12</sub>O<sub>40</sub> has a good degradation capacity for PR as compared to MgAl-PW<sub>12</sub>O<sub>40</sub>, ZnAl-SiW<sub>12</sub>O<sub>40</sub>, and ZnAl-PW<sub>12</sub>O<sub>40</sub>. The result shows that the LDH composite presents stability and has good photocatalytic activities toward the reduction of methylene blue. The materials utilized for the fifth regeneration are indicated by the FTIR results, which verified the LDH composite structure. The photodegradation process of procion red for immaculate ZnAl-LDH, MgAl-LDH, ZnAl-[PW<sub>12</sub>O<sub>40</sub>], ZnAl-[SiW<sub>12</sub>O<sub>40</sub>], MgAl-[PW<sub>12</sub>O<sub>40</sub>], MgAl-[SiW<sub>12</sub>O<sub>40</sub>] amounted to 68%, 70%, 56%, 79%, 74%, and 80%, respectively. The capacity of LDH-polyoxometalate composite material to successfully photodegrade, as measured by the percentage of degradation, revealed an increase in photodegradation catalysis and the ability of LDH to regenerate.

**Keywords:** polyoxometalate, LDH, photocatalytic, methylene blue.

### INTRODUCTION

Currently, researchers focus on pollution control, especially wastewater treatment, to answer environmental control of textile, paper, petroleum, and agriculture manufacturing. The wastewater pollutants are mostly organic dyes, which contain high concentrations of organic pollutants. Aquatic systems may be exposed to wastewater with intense color and toxicity. The structure of the dye contains an aromatic ring that is harmful to the environment (Arumugham et al., 2018). Among them are the azo dyes with the azo group

-N=N-, which are also recognized to be harmful for the environment due to toxic materials and their ability to cause cancer in humans and pollution in oceans, lakes, and rivers (de Almeida et al., 2021). The common techniques for treating dye wastewater include biological and chemical procedures (Sirianuntapiboon et al., 2007). Biological wastewater treatment when compared to other treatment options, is frequently the least expensive. However, it is thought that dyes are resistant to biodegradation (J. Zhang et al., 2020). Because the decay rates heavily depend on the reactivity and photosensitivity of a dye, direct

photolysis of organic dyes in the natural environment has proven to be challenging (Neppolian et al., 2002). No treatment method now in use is 100 percent successful, and some call for the use of several different strategies.

The conventional treatment applied for wastewater pollutants, such as the adsorption process, coagulation, and membrane separation remains to be solved by the degradation problem. Effective alternative treatments are needed. Recent efforts included developing the degradation treatment based on the presence of UV irradiation. The last ten years have seen considerable advancements in the photocatalysis process, which has generated a great deal of attention. The photocatalytic process has generated a great deal of attention. The photocatalytic process also offers an intriguing benefit for this kind of pollution; in fact, the direct mineralization of the azo group is the perfect example of environmental treatment, because it results in the synthesis of an element that makes up the atmosphere.

The dye in wastewater can be eliminated by UV irradiation and nano-sized  $\text{TiO}_2$  powder (Ali et al., 2021). TOC is the most effective method of cleaning up wastewater contaminated with procion red mx-5b (Cotillas et al., 2018) (Figure 1). EDTA-modified  $\text{BiFeO}_3$  reached 70% degradation of procion red (Da Cruz Severo et al., 2020). Lin and Lee., (2010)  $\text{TiO}_2/\text{Ag}$  materials that have been created demonstrate effective photocatalysis. At the same time, Costa et al., (2004) achieved 93% resulting color for the red and yellow dyestuffs by the photodegradation process.

Among all the various materials, LDH has been promoted for photocatalyzed pollutant degradations because of its stability, large surface area, adjustable band gap, remarkable recyclability, and high anion exchange capacity (Zhang et al., 2019). Layered double hydroxides (LDHs) are ionic layered structures with the general formula  $[\text{M}^{\text{II}}_{1-x}\text{M}^{\text{III}}_x(\text{OH})_2]^{x+}[(\text{A}^{\text{n-}})_{x/n}\cdot y\text{H}_2\text{O}]^{x-}$  (Birjega et al.,

2016). LDHs have been used extensively and are regarded as powerful adsorbents for removing anionic dyes (Lafi et al., 2016). However, due to the difficulty in separating the treated dye solution from the spent LDH, their use is restricted (Clark et al., 2019). NiAlCe-LDH successfully degraded organic dye and reached 100% (Tao et al., 2019). Moreover, LDH variant which is NiFe-LDH have been proposed for better photocatalytic performance of photocatalysts (Wu et al., 2020). Liu et al., (2016) successfully constructed an indirect photocatalytic heterostructure system comprising  $\text{ZnIn}_2\text{S}_4/\text{Au}/\text{g-C}_3\text{N}_4$  for NO removal and  $\text{CO}_2$  reduction. According to Yuliasari et al., (2022) modified Zn, Mg/Al-LDH with metal oxide as a catalyst for decomposing malachite green was reported to have superior performance to LDH.

In the present study, LDH composite Mg/Zn LDH and Mg/Zn were modified with two different polyoxometalates (POM) type Keggin  $\text{K}_4[\alpha\text{-SiW}_{12}\text{O}_{40}]$  and  $\text{K}_3[\alpha\text{-PW}_{12}\text{O}_{40}]$  and used as a photocatalyst. The investigated photodegradation factors included the impact of pH, catalyst loading, contact time, and recycled breakdown material. The selected polyoxometalate compound as intercalated with Mg/Zn LDH as intercalation due to polyoxometalate has a high negative charge that can increase the capacity for performance on degrading dye, which can make procion red photodegradation. Figure 1 shows the structure of procion red dye. The XRD, FTIR, SEM, and UV-DRS were used to characterize the prepared and synthesized material.

## EXPERIMENT

### Chemicals and instrumentation

The study made use of sodium phosphate, sodium tungstate, sodium carbonate, magnesium nitrate, zinc nitrate, aluminum nitrate sodium hydroxide, and hydrogen chloride. One of the

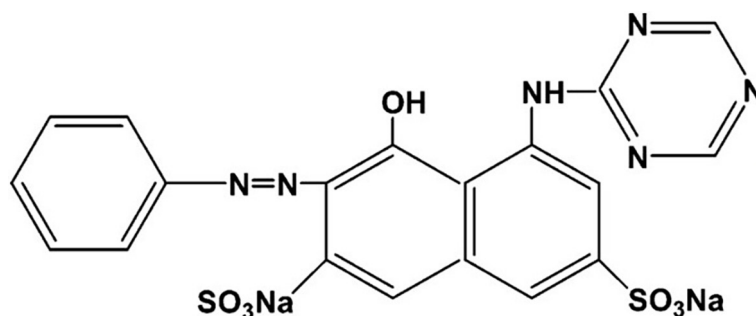


Figure 1. The structures of the procion red

synthetic dyes, procion red mx-5B, has formula  $C_{19}H_{10}Cl_2N_6Na_2O_7S_2$  and maximum absorbance at  $\lambda_{max}$  615 nm. A Rigaku XRD Miniflex-6000 diffractometer was used to characterize the materials. Shimadzu FTIR Prestige-21 performed FTIR analysis. The UV-Vis Biobase BK-UV 1800 PC spectrophotometer was used to measure the degradation of PR between 660–668 nm. Diffuse UV-Vis Reflectance Spectrometer JASCO V-760 was used for band gap analysis, while SEM FEI Quanta 650 was used for morphology analysis.

## CATALYST SYNTHESIS AND PREPARATION

### Synthesis of Mg/Zn LDH

LDH precursors eventually achieved the layered structure after being agitated in water with water combining into the structure to form the LDH phase (Wang, 2016). Both Mg and Zn LDH were generated using a modified co-precipitation. The details are as follows: an amount of magnesium nitrate 18.75 g was mixed in water and aluminum nitrate 9.3 g was dissolved in a water stirrer for 2 hours. Sodium hydroxide was added to the mixture to bring the pH level reach to pH 10. This mixture was stirred for 6 hours at 85 °C; then, MgAl LDH was weighed. A two-step synthesis of ZnAl-LDH by adding 0.25 M aluminium nitrate and 0.75 M zinc nitrate, the addition of sodium hydroxide to reach pH 8, then stirred up to 18 hours at 85 °C.

### Preparation of catalyst composite

Mg/Zn LDH is modified with a polyoxometalate compound, Keggin  $K_4[\alpha-SiW_{12}O_{40}]$  and  $K_3[\alpha-PW_{12}O_{40}]$ . The composite was mixed by adding 1 g polyoxometalate and 2 g LDH with adding sodium hydroxide 1 M. The suspensions were created fast for two days while being exposed to  $N_2$  gas for 2 days. Then, the suspension dried after being washed at a temperature of 80°C for 12 hours. XRD, FTIR, SEM, and UV-DRS were used to characterize materials.

### Photocatalytic activity

In a 20 mg/L procion red, the initial step that was to place it under the dark conditions and agitate for 30 minutes on magnetically a desorption equilibrium; then, the photocatalytic activity of the sample was assessed. The photodegradation

process applied at degradation optimization involves pH range fluctuations (3, 5, 7, 9, and 11), catalyst loading at 0.02, 0.04, 0.06, 0.08, and 0.1 g, and for the contact time degradation at 10, 20, 30, 40, 50, 60, 70, 80, 90, 100, 110, and 120 minutes. Utilizing UV light, this photodegradation process was carried out. The following equation formula is used to define the percentage of degradation (%) =  $(C_0 - C_t)/C_0 \times 100$ ,  $C_0$  is the dye concentration at the start of the degradation process, and  $C_t$  is the dye concentration after degradation has finished (Hadnadjev-Kostic et al., 2017).

### Regeneration experiment

To determine the photocatalyst repeatability, the solution and the suspension were separated by a precipitate. The precipitate powder was then dried for 24 h at 70 °C. The photocatalytic reaction was carried out on the solid powder. To confirm the reproducibility of both the pristine LDH and LDH composite photocatalyst, the above method was carried out a fifth time.

## RESULTS AND DISCUSSION

### Analysis and characterization of catalyst

The XRD patterns of the prepared MgAl-LDHs, ZnAl-LDHs, MgAl-PW<sub>12</sub>O<sub>40</sub>, MgAl-SiW<sub>12</sub>O<sub>40</sub>, ZnAl-PW<sub>12</sub>O<sub>40</sub>, and ZnAl-SiW<sub>12</sub>O<sub>40</sub> were shown in Figure 2. As shown in Figure 2, the diffraction peak of both pristine LDH MgAl-LDHs and ZnAl-LDHs can be detected at approximately  $2\theta = 10.39^\circ, 20.17, 34.6$  and  $60.32$  all coincide with the LDHs structure which is similar to the crystal plane at (003), (006), (009) and (110). The crystallinity of the material is pristine, as evident by the sharp diffraction peaks. The XRD pattern of the material composite is shown in Figure 2. The peaks at  $2\theta$  and crystal plane = 11.80 (003), 23.59 (006), 31.90 (009), 46.74 (015), and 61.7 (110), respectively, for MgAl-PW<sub>12</sub>O<sub>40</sub> the same kind LDH which is MgAl-LDH intercalated SiW<sub>12</sub>O<sub>40</sub> showed diffraction peak at 8.41, 25.07 and 34.60. Furthermore, composited material on ZnAl-PW<sub>12</sub>O<sub>40</sub> showed a bit more peak diffraction than ZnAl-SiW<sub>12</sub>O<sub>40</sub>. ZnAl-SiW<sub>12</sub>O<sub>40</sub> observed at  $2\theta = 8.16, 25.27, 33.8,$  and  $66.3$ , corresponding to the crystal planes (003), (006), (015), and (110). ZnAl-PW<sub>12</sub>O<sub>40</sub> showed at peak 7.73, 28.6 and 35.6. In this research, it was found that the involvement of polyoxometalate is supported in LDH layers.

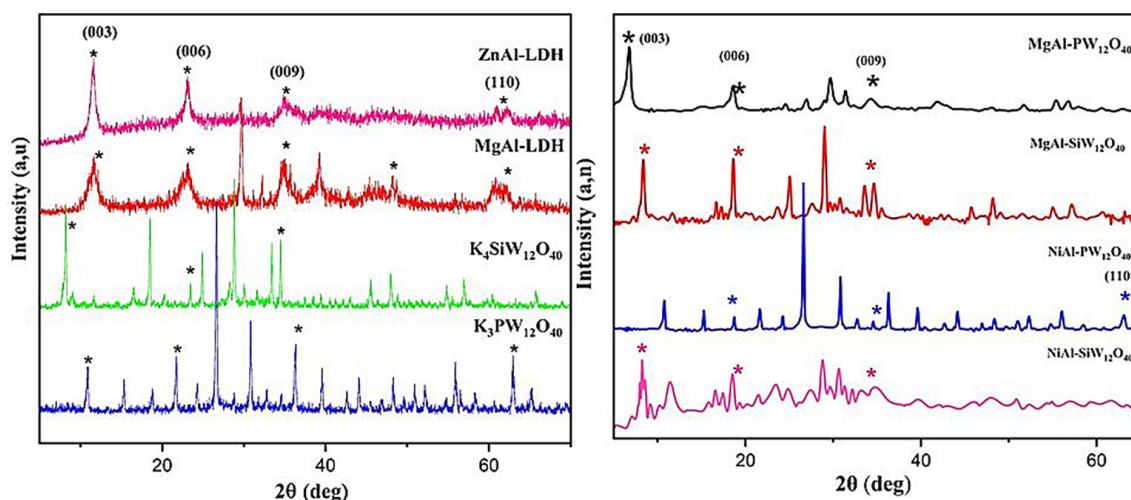


Figure 2. Diffractogram of the catalyst

### FTIR characterization

Raman spectrum was performed to analyze the molecular vibration of pristine LDH, LDH composite, and polyoxometalate compound. The O-H stretching vibration corresponds to the absorption band at  $2917\text{ cm}^{-1}$ . The vibration of  $\text{H}_2\text{O}$  showed  $1735\text{ cm}^{-1}$ . The value of  $1399\text{ cm}^{-1}$  corresponds to  $\text{CO}_3^{2-}$ . The low wavenumber from  $400 - 800\text{ cm}^{-1}$  can be attributed to the metal hydroxide sheets in the brucite-like lattice (M-O and O-M-O) (Li et al., 2018). The FTIR spectrum of polyoxometalate contains bands at  $925\text{--}789\text{ cm}^{-1}$  (W-O-W),  $979\text{ cm}^{-1}$  (W=O),  $1020\text{ cm}^{-1}$  (W-O) (Lesbani & Mohadi, 2014). Mirzaei et al., (2019) interpreted  $\alpha$ -Keggin  $\text{SiW}_{12}$  at bands  $813, 882, 927,$  and  $973\text{ cm}^{-1}$  for W-O. LDH intercalated polyoxometalate compound, the spectrum of the LDH composite showed the successfully modified by showing the absorption band at  $794 - 547\text{ cm}^{-1}$ .

Figure 3 shows that generally, LDH composites were maintained by being supported with polyoxometalate. The characteristic vibration disappeared, whereas the vibration of LDHs was preserved; it indicated that the layered structures of polyoxometalate were dissolved.

### Structural analysis

Figure 4 shows the representative SEM image of LDH composite and pristine LDH can be seen with morphology consisting of dominant nanoparticles, noticeably the aggregation of the LDH composite happens, and the EDX of both pristine material and material composite is shown in Table 1. Pristine material and material composite indicates the atomic ratio of LDH and polyoxometalate of 2:1. The SEM image of  $\text{MgAl-SiW}_{12}\text{O}_{40}$  is shown in Figure 4e the

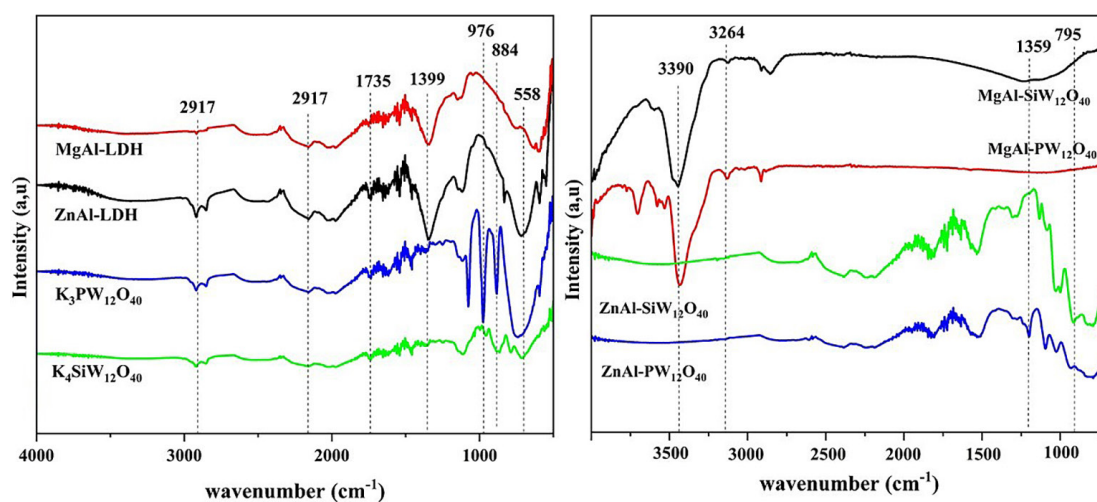


Figure 3. FTIR spectra of pristine LDH and LDH composite

**Table 1.** EDX of pristine material

Element	MgAl-HLG (%wt)	ZnAl-HLG (%wt)	K <sub>4</sub> -SiW <sub>12</sub> O <sub>40</sub> (%wt)	K <sub>3</sub> -PW <sub>12</sub> O <sub>40</sub> (%wt)
Mg	8.14	2.51	88.3	4.9
Al	5.20	1.62	1.3	1.7
W	-	32.54	-	44.7
P	-	7.82	-	0.7
Si	-	-	-	-
K	-	3.53	-	2.7
Cl	-	9.17	-	-
C	13.57	8.20	-	14.5
O	51.39	28.78	9.1	25.6
Na	2.58	5.83	-	4.9
N	9.12	-	1.4	-

**Table 2.** EDX of material composite

Element	MgAl-Pw (%wt)	MgAl-Si (%wt)	ZnAl-Pw (%wt)	ZnAl-Si (%wt)
Mg	6.32	2.51	-	-
Al	6.85	1.62	5.47	3.81
W	2.15	32.54	1.10	3.14
P	7.82	-	2.43	-
Si	-	-	-	0.91
K	-	3.53	-	0.61
Cl	-	9.17	-	15.68
C	7.98	8.20	11.6	14.68
O	45.85	28.78	48.2	41.52
Na	4.1	5.83	15.59	12.42
Zn	-	-	-	9.23
N	-	-	11.02	13.68

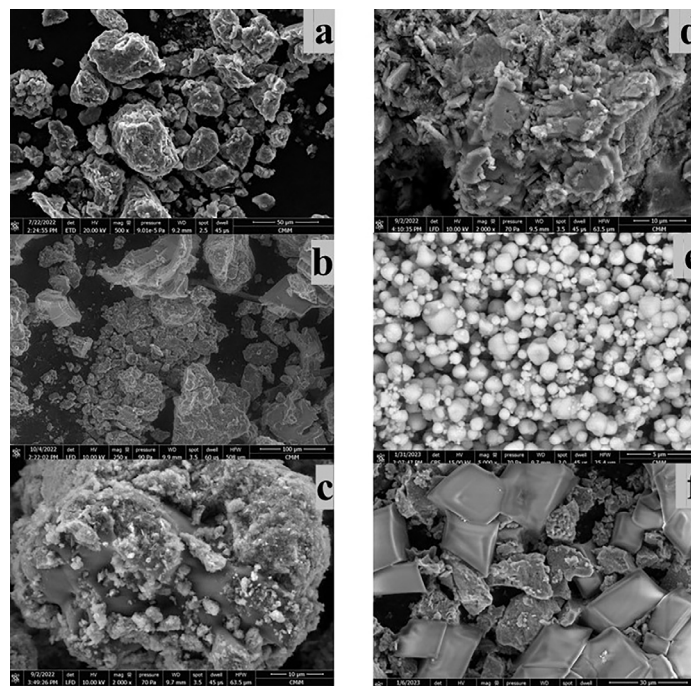


**Figure 4.** SEM Analysis of MgAl-LDH (a) ZnAl-LDH (b) MgAl-SiW<sub>12</sub>O<sub>40</sub> (c) MgAl-PW<sub>12</sub>O<sub>40</sub> (d) ZnAl-SiW<sub>12</sub>O<sub>40</sub> (e) and ZnAl-PW<sub>12</sub>O<sub>40</sub> (f)

polyoxometalate appears in the small particle that sticks on the surface of MgAl-LDH. The material in this study shows a small size with a heterogeneous shape and aggregate formation. In turn, the EDX spectrum in Table 1 and Table 2 of the prepared material revealed the atomic ratio of Mg and Zn expected the composite resulting in the same amount of precursor was used; the atomic percentage of O is almost the same after being composed LDH with polyoxometalate.

### Effect of catalyst dosage

The effect of the pristine material (MgAl-LDH and ZnAl-LDH) and composite material (MgAl-PW<sub>12</sub>O<sub>40</sub>, MgAl-SiW<sub>12</sub>O<sub>40</sub>, ZnAl-PW<sub>12</sub>O<sub>40</sub>, and ZnAl-SiW<sub>12</sub>O<sub>40</sub>) dosage (0.02; 0.04; 0.06; 0.08 and 0.1 g) on the degradation efficiency of procion red was investigated (as shown in Figure 5) the initial concentration of procion red was

20 mg/L and for the pH of the solution was not adjusted. It can be seen that the degradation was efficiently enhanced by the increased catalyst dosage, based on Figure 5, the highest increase reached 91% of procion red degradation. It is because the more catalyst added the more radicals can be generated for photodegradation dye. Thus, the photocatalytic can efficiently involve.

### Effect of initial pH

The surface characteristics of the catalyst are affected by the pH level of the solution; this can enhance the ionization of procion red dye and the production of active radicals. The original pH value of the solution was pH, 3, 5, 7, 9, and 11 with a 20 mg/L catalyst dosage. Figure 6 illustrates how the degrading effectiveness and reaction rate constant varied as the initial pH increased. At pH 1, the removal effectiveness increased for MgAl-Si

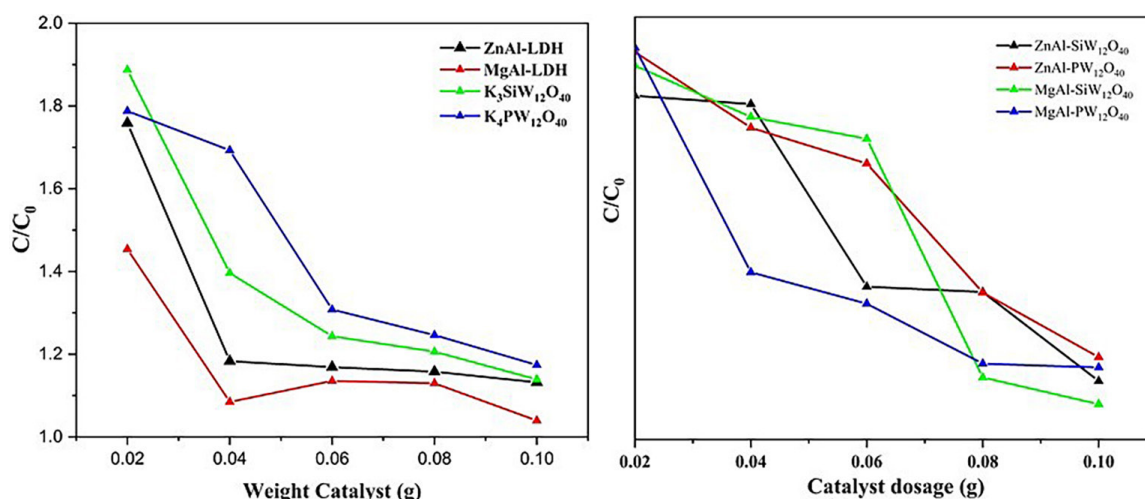


Figure 5. Effect of catalyst weight on degradation procion red

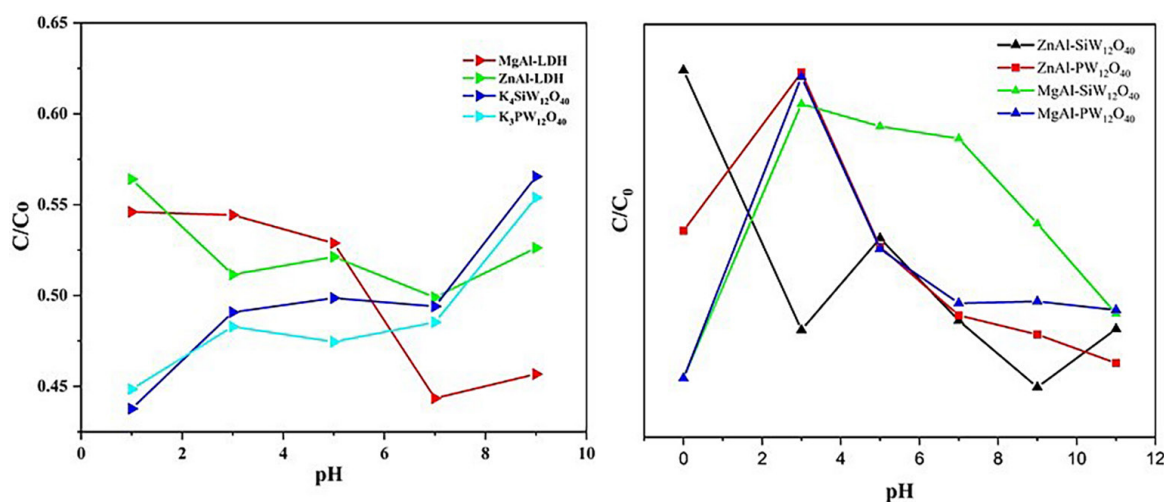


Figure 6. Effect of pH on degradation procion red

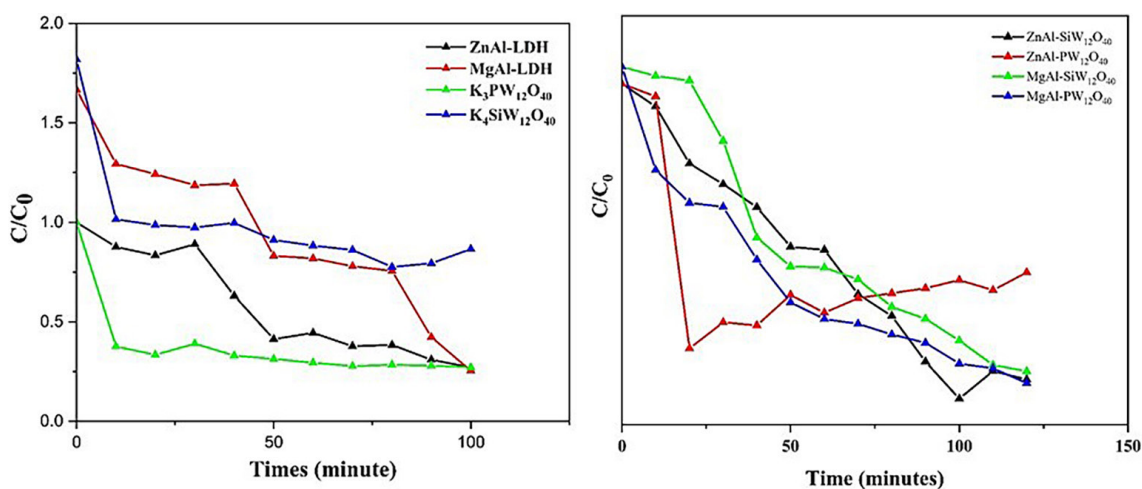


Figure 7. Effect of time on the degradation of procion red

$W_{12}O_{40}$ , and  $ZnAl-SiW_{12}O_{40}$ , pH 5 for  $ZnAl-LDH$ , pH 7 for  $MgAl-LDH$  and  $MgAl-PW_{12}O_{40}$ , and pH for  $ZnAl-PW_{12}O_{40}$ . Hu et al., (2019) reported that rising  $C_{(OH)^-}$  level in solution caused the increased rate of the degradation process, due to promoting the production of an OH radical based on  $OH^- + h^+$  to OH radicals.

### Effect of reaction time

The analysis and evaluation of the synthesized material's photocatalytic capability due to the degradation of reaction time under visible light. Figure 7 presents the results of the pristine material and composite material, where composite material exhibits great photodegradation efficiency. 20 mg/L of catalyst was employed in the solution to study the effects of time degradation at 2 hour reaction periods. The higher value of converting the procion red dye on the degradation process was determined by detecting an increase in reaction time. The highest reaction time was extended for one or more hours, the more efficient degradation process, which is the amount of procion red degraded. The percentage degradation of procion red of  $MgAl-LDH$ ,  $ZnAl-LDH$ ,  $ZnAl-[PW_{12}O_{40}]$ ,  $ZnAl-[SiW_{12}O_{40}]$ ,  $MgAl-[PW_{12}O_{40}]$ ,  $MgAl-[SiW_{12}O_{40}]$  was 68%, 70%, 56%, 79%, 74%, and 80%, respectively.

### Acknowledgments

The authors thank the Research Center of Inorganic Materials and Complexes FMIPA Universitas Sriwijaya for valuable discussion, apparatus, and chemical analysis.

### REFERENCES

1. Ali, H.T., Mateen, A., Ashraf, F., Javed, M.R., Ali, A., Mahmood, K., Zohaib, A., Amin, N., Ikram, S., Yusuf, M. 2021. A new SERS substrate based on Zn-2GeO4 nanostructures for the rapid identification of E.Coli and methylene blue. *Ceramics International*, 47(19), 27998–28003.
2. Arumugham, T., Kaleekkal, N.J., Rana, D. 2018. Fabrication of novel aromatic amine functionalized nanofiltration (NF) membranes and testing its dye removal and desalting ability. *Polymer Testing*, 72, 1–10.
3. Birjega, R., Vlad, A., Matei, A., Ion, V., Luculescu, C., Dinescu, M., Zavoianu, R. 2016. Growth and characterization of ternary Ni, Mg–Al and Ni–Al layered double hydroxides thin films deposited by pulsed laser deposition. *Thin Solid Films*, 614, 36–41.
4. Clark, I., Smith, J., Gomes, R. L., Lester, E. 2019. Continuous Synthesis of  $Zn_2Al-CO_3$  Layered Double Hydroxides for the Adsorption of Reactive Dyes from Water. *Journal of Environmental Chemical Engineering*, 7(3).
5. Costa, F.A.P., dos Reis, E.M., Azevedo, J.C.R., Nozaki, J. 2004. Bleaching and photodegradation of textile dyes by  $H_2O_2$  and solar or ultraviolet radiation. *Solar Energy*, 77(1), 29–35.
6. Cotillas, S., Clematis, D., Cañizares, P., Carpanese, M.P., Rodrigo, M.A., Panizza, M. 2018. Degradation of dye Procion Red MX-5B by electrolytic and electro-irradiated technologies using diamond electrodes. *Chemosphere*, 199, 445–452.
7. Da Cruz Severo, E., Dotto, G.L., Silvestri, S., Dos Santos Nunes, I., Da Silveira Salla, J., Martinez-De La Cruz, A., Da Boit Martinello, K., Foletto, E.L. 2020. Improved catalytic activity of EDTA-modified  $BiFeO_3$  powders for remarkable degradation

- of procion red by heterogeneous photo-Fenton process. *Journal of Environmental Chemical Engineering*, 8(4).
8. de Almeida, E.J.R., Halfeld, G.G., Reginatto, V., de Andrade, A. R. 2021. Simultaneous energy generation, decolorization, and detoxification of the azo dye Procion Red MX-5B in a microbial fuel cell. *Journal of Environmental Chemical Engineering*, 9(5).
  9. Hadnadjev-Kostic, M., Vulic, T., Marinkovic-Neducin, R., Lončarević, D., Dostanić, J., Markov, S., Jovanović, D. 2017. Photo-induced properties of photocatalysts: A study on the modified structural, optical and textural properties of TiO<sub>2</sub>-ZnAl layered double hydroxide based materials. *Journal of Cleaner Production*, 164, 1–18.
  10. Hu, Y., Li, H., Wang, Q., Zhang, J., Song, Q. 2019. Characterization of LDHs prepared with different activity MgO and resisting Cl<sup>-</sup> attack of concrete in salt lake brine. *Construction and Building Materials*, 229.
  11. Lafi, R., Charradi, K., Djebbi, M.A., Ben Haj Amara, A., Hafiane, A. 2016. Adsorption study of Congo red dye from aqueous solution to Mg-Al-layered double hydroxide. *Advanced Powder Technology*, 27(1), 232–237.
  12. Lesbani, A., & Mohadi, R. 2014. Brønsted acid of Keggin type polyoxometalate catalyzed pinacol rearrangement. *Bulletin of Chemical Reaction Engineering and Catalysis*, 9(2), 136–141.
  13. Lin, Y.C., Lee, H.S. 2010. Effects of TiO<sub>2</sub> coating dosage and operational parameters on a TiO<sub>2</sub>/Ag photocatalysis system for decolorizing Procion red MX-5B. *Journal of Hazardous Materials*, 179(1–3), 462–470.
  14. Liu, C.G., Zheng, T., Liu, S., Zhang, H.Y. 2016. Photodegradation of malachite green dye catalyzed by Keggin-type polyoxometalates under visible-light irradiation: Transition metal substituted effects. *Journal of Molecular Structure*, 1110, 44–52.
  15. Mirzaei, M., Eshtiagh-Hosseini, H., Hassanpoor, A. 2019. Different behavior of PDA as a preorganized ligand versus PCA ligand in constructing two inorganic-organic hybrid materials based on Keggin-type polyoxometalate. *Inorganica Chimica Acta*, 484, 332–337.
  16. Neppolian, B., Jung, H., Choi, H., Lee, J.H., Kang, J.W. 2002. Sonolytic degradation of methyl tert-butyl ether: the role of coupled fenton process and persulphate ion. In *Water Research* (Vol. 36).
  17. Sirianuntapiboon, S., Sadahiro, O., Salee, P. 2007. Some properties of a granular activated carbon-sequencing batch reactor (GAC-SBR) system for treatment of textile wastewater containing direct dyes. *Journal of Environmental Management*, 85(1), 162–170.
  18. Tao, X., Han, Y., Sun, C., Huang, L., & Xu, D. 2019. Plasma modification of NiAlCe-LDH as improved photocatalyst for organic dye wastewater degradation. *Applied Clay Science*, 172, 75–79.
  19. Wu, Y., Gong, Y., Liu, J., Chen, T., Liu, Q., Zhu, Y., Niu, L., Li, C., Liu, X., Sun, C.Q., Xu, S. 2020. Constructing NiFe-LDH wrapped Cu<sub>2</sub>O nanocube heterostructure photocatalysts for enhanced photocatalytic dye degradation and CO<sub>2</sub> reduction via Z-scheme mechanism. *Journal of Alloys and Compounds*, 831.
  20. Yuliasari, N., Wijaya, A., Amri, Mohadi, R., Elfita, Lesbani, A. 2022. Application of M<sup>2+</sup> (Magnesium, Zinc)/Alumina-Metal Oxide Composites as Photocatalysts for the Degradation of Cationic Dyes. *Ecological Engineering and Environmental Technology*, 23(4), 125–135.
  21. Zhang, J., Zhu, Q., Wang, L., Nasir, M., Cho, S.H., Zhang, J. 2020. g-C<sub>3</sub>N<sub>4</sub>/CoAl-LDH 2D/2D hybrid heterojunction for boosting photocatalytic hydrogen evolution. *International Journal of Hydrogen Energy*, 45(41), 21331–21340.
  22. Zhang, L., Gong, Z., Jiang, B., Sun, Y., Chen, Z., Gao, X., Yang, N. 2019. Ni-Al layered double hydroxides (LDHs) coated superhydrophobic mesh with flower-like hierarchical structure for oil/water separation. *Applied Surface Science*, 490, 145–156.